

Depinning of domain walls in notched antiferromagnetic nanowires

Z. Y. Chen¹, M. H. Qin^{1,*}, and J. –M. Liu²

¹*Institute for Advanced Materials, South China Academy of Advanced Optoelectronics and Guangdong Provincial Key Laboratory of Quantum Engineering and Quantum Materials, South China Normal University, Guangzhou 510006, China*

²*Laboratory of Solid State Microstructures and Innovative Center for Advanced Microstructures, Nanjing University, Nanjing 210093, China*

[Abstract] In this work, we study the domain wall pinning at a notch in antiferromagnetic (AFM) nanowires theoretically and numerically. The depinning fields depending on the notch size and internal parameters are calculated theoretically and numerically. Contrary to the conventional conception, the depinning field gradually increases to a saturation value with the increase of the damping constant. This phenomenon is explained analytically based on one-dimensional model, which attributes to the internal dynamics of the domain wall. More interestingly, our work demonstrates that the depinning mechanism of AFM domain walls is different from that of ferromagnetic domain walls, and the former depinning could be typically three orders faster than the latter, confirming again the ultrafast dynamics of AFM systems.

Keywords: antiferromagnetic dynamics, domain wall, lattice defect, pinning effect

Antiferromagnetic (AFM) materials are promising materials for future AFM spintronics devices and attract more and more attentions especially because they have strong anti-interference capability and ultrafast magnetic dynamics.¹⁻⁸ As a frontier and highly concerned major issue for advanced spintronics, the domain dynamics of antiferromagnets has been extensively investigated. Specifically, several stimuli have been proposed numerically and theoretically to drive the domain wall (DW) motion, including the Néel spin-orbit torques,⁹⁻¹⁰ spin waves,¹¹⁻¹² temperature gradients¹³⁻¹⁵ and so on.¹⁶⁻¹⁸ These important works indeed provide useful information for future storage device design.

Nevertheless, most of these works investigated the models for perfect samples and neglected the pinning of DWs caused by disorder and local defects. As a matter of fact, the pinning of domain walls (DWs) may play an important role in understanding magnetic dynamics. On the one hand, for a realistic spintronic device where inhomogeneity and lattice defects are inevitable, the domain dynamics could be significantly affected. For example, it has been experimentally reported that the electrical current induced switching of AFM domains in CuMnAs occurs only in localized regions, strongly suggesting the important role of the pinning of DWs.¹⁹ Thus, the physical mechanisms deserve to be clarified in order to understand the experimental report better. On the other hand, artificial lattice defects such as notches with proper shapes could be used in discretizing the DW position and enhancing the stability of DWs against thermal fluctuations and stray fields in potential racetrack memory and logic devices.²⁰⁻²⁴ So, the study of the pinning of AFM DWs is essential both in application potential and in basic physical research.

Fortunately, the pinning effects of ferromagnetic (FM) DWs have been extensively investigated, and the accumulated experience can be partially transferred to the study of AFM domain dynamics.²⁵⁻³² For example, through minimizing the energy of FM system, the depinning field has been derived analytically, clearly demonstrating the important role of the notch geometry and DW structures in the pinning of DWs.²⁶ More interestingly, the dependence of the depinning field on the Gilbert damping has been revealed in recent micromagnetic simulations, i. e. a small damping constant reduces the depinning field, contrary to the general expectation that they should be independent of each other.²⁷ Based on the one-dimensional model, the simulated results are explained in terms of the internal

dynamics of DWs including spin precession, demonstrating the complexity of the DW pinning.

In this work, we study the DW pinning at a notch in an AFM nanowire. The depinning fields depending on the notch size and uniaxial anisotropy are calculated theoretically, which are well consistent with the numerical simulations. Moreover, with the increase of the damping constant, the depinning field gradually increases to a saturation value. This phenomenon is well explained by the analysis of one-dimensional model considering the internal dynamics of the DW. More interestingly, our work demonstrates a different depinning mechanism of the AFM DW and suggests that the depinning could be typically three orders faster than that in FM system.

We study the pinning of DW at a notch in an AFM nanowire with length l along the z -axis, width w and thickness t_l . As an example, the current induced Néel spin-orbit torques (or staggered effective field) available in CuMnAs and Mn₂Au are used to drive the DW motion.^{6,8-9} The model Hamiltonian density is given by³³⁻³⁴

$$H = \frac{A_0}{2} \mathbf{m}^2 + \frac{A}{2} \nabla \mathbf{n} \cdot \nabla \mathbf{n} + L_0 \mathbf{m} \cdot \nabla \mathbf{n} - \frac{K_z}{2} n_z^2 + \gamma \rho h n_z, \quad (1)$$

where $A_0 = 4JS^2/a$ is the homogeneous exchange constant with AFM coupling $J > 0$, the spin length S and lattice constant a , \mathbf{m} is the total magnetization $\mathbf{m} = (\mathbf{m}_1 + \mathbf{m}_2)/2S$ with \mathbf{m}_1 and \mathbf{m}_2 are the sublattice magnetizations, $A = 2aJS^2$ is the inhomogeneous exchange constant, \mathbf{n} is the staggered magnetization $\mathbf{n} = (\mathbf{m}_1 - \mathbf{m}_2)/2S$, $L_0 = 2JS^2$ is the parity-breaking parameter, $K_z = 2d_z S^2/a$ is the anisotropy constant along the z -axis in the continuum model with the anisotropy constant d_z in the discrete model, γ is the gyromagnetic ratio, $\rho = S\hbar/a$ is the density of the staggered spin angular momentum per unit cell, h is the staggered effective field and n_z is the z component of \mathbf{n} . Here, we introduce a notch with width d and depth w_N into the nanowire to simulate lattice defect, as depicted in Fig. 1(a).

Noting that \mathbf{m} is just a slave variable of \mathbf{n} ,³³ we eliminate \mathbf{m} by $\mathbf{m} = -L_0 \nabla \mathbf{n} / A_0$ and obtain

$$H = \frac{A^*}{2} \nabla \mathbf{n} \cdot \nabla \mathbf{n} - \frac{K_z}{2} n_z^2 + \gamma \rho h n_z, \quad (2)$$

where $A^* = A - L_0^2/A_0$ is the effective exchange constant. After a similar derivation, the

depinning field for AFM DWs is given by²⁶

$$h_{dep} = \frac{2d_z / \mu_s}{2w/w_N - 1}, \quad (3)$$

where μ_s is the saturation moment (see Supplementary Material for detailed derivation). It's noted that for an ultra-thin nanowire, the depinning field is independent of the thickness.

In order to check the validity of Eq. 3, we also perform the numerical simulations based on the atomistic Landau-Lifshitz-Gilbert (LLG) equation,¹⁴

$$\frac{\partial \mathbf{S}_i}{\partial t} = -\frac{\gamma}{(1+\alpha^2)} \mathbf{S}_i \times [\mathbf{H}_i + \alpha(\mathbf{S}_i \times \mathbf{H}_i)], \quad (4)$$

where \mathbf{S}_i is the normalized atomic spin at site i , α is the damping constant, $\mathbf{H}_i = -\mu_s^{-1} \partial H / \partial \mathbf{S}_i$ is the effective field. Unless stated elsewhere, $l = 120a$, $t_l = a$, $w = 8a$, $d_z = 0.02J$, $d = 4a$, $w_N = 2a$ and $\alpha = 0.02$ are selected.

Fig. 1 presents the spin structures of the nanowire for various h . Under zero h , the DW structure is symmetric around the notch due to the absence of chirality, as shown in Fig. 1(a). When a small h is applied, the DW slightly shifts toward the right side and finally be pinned by the lattice defect. Specifically, h tends to array the spins in the cross section (xy plane) at EF parallel to the plane, as shown in Figs. 1(b) and 1(c). As a matter of fact, Eq. (3) is derived based on the assumption that under the depinning field, the spins in the cross section are perfectly parallel to the xy plane. As h increases above the depinning field ~ 0.0042 , the DW could get over the potential well generated by the lattice defect and be efficiently driven by the field (Fig. 1(d)).

Subsequently, we investigate the dependences of the depinning field on the notch geometry and other parameters including the anisotropy and damping constants, and give the numerical and analytical results in Fig. 2. It is noted that the potential well generated by the notch significantly increases with the increase of the notch size, and large field is needed to depin the DWs. As a result, with the increasing w_N/w , h_{dep} obviously increases/decreases, as clearly shown in Fig. 2(a)/2(b). On the other hand, the total energy of the DW E_{DW} determines the mobility of the DW, specifically, higher energy leads to a lower mobility. Thus, E_{DW} increases with the increase of d_z , and large field is needed to get the DW out of the potential well, as confirmed in Fig. 2(c) which presents the calculated h_{dep} as a function of d_z .

So far, the simulated results are well consistent with the analytical results. However, the consistency is challenged in the studied α -dependent h_{dep} , as shown in Fig. 2(d). In Eq. 3, h_{dep} is independent of α . However, the numerical simulation clearly demonstrates that h_{dep} increases with α and finally reaches to a saturation value. It is noted that in the derivation of Eq. 3, the internal dynamics of DWs has been completely neglected, which affects the calculations especially for small damping constants.

In order to uncover the intriguing physics behind this phenomenon, we record the position of the DW as a function of time t for various α in Fig. 3(a). Here,³⁵ similar to the well-studied skyrmions, the position of the DW center $q(t)$ is estimated by

$$q = \frac{\int z(1-|n_z|)dxdz}{\int (1-|n_z|)dxdz}. \quad (5)$$

For large $\alpha > 0.005$, the DW just oscillates around the equilibrium position with an attenuating amplitude. Moreover, the oscillation amplitude is enhanced with the decreasing α . Finally, when the maximum displacement of the DW ($|\Delta q|_{\text{max}} = |q(t) - q(0)|_{\text{max}}$) exceeds the length of the pinning potential,²⁹ the DW depins from the notch and propagates freely along the nanowire.

Subsequently, we do further analytical calculations based on one-dimensional model considering the internal dynamics of DWs to reveal the physical mechanisms in more details.²⁸⁻²⁹ The Hamiltonian density in one-dimensional model reads³³

$$H_{1D} = \frac{A_0}{2} \mathbf{m}^2 + \frac{A}{2} (\partial_z \mathbf{n})^2 + L_0 \mathbf{m} \cdot \partial_z \mathbf{n} - \frac{K_z}{2} n_z^2 + \gamma \rho h n_z + V(z), \quad (6)$$

where the pinning effects of the notch is described by the potential energy $V(z)$. In the following step, we study the Lagrangian density $L = K - H_{1D}$ with $K = \rho \mathbf{m} \cdot (\dot{\mathbf{n}} \times \mathbf{n})$ is the kinetic energy term introduced by the Berry phase, and $\dot{\mathbf{n}}$ represents the derivative with respect to time.^{33,36-37} Then, we eliminate \mathbf{m} with $\mathbf{m} = (\rho \dot{\mathbf{n}} \times \mathbf{n} - L_0 \partial_z \mathbf{n})/A_0$,³³ and obtain

$$L = \frac{\rho^2}{2A_0} \dot{\mathbf{n}}^2 - \frac{A^*}{2} (\partial_z \mathbf{n})^2 + \frac{K_z}{2} n_z^2 - \gamma \rho h n_z - V(z). \quad (7)$$

To describe the dissipative dynamics, the Rayleigh function density $R = \alpha \rho \dot{\mathbf{n}}^2/2$ is introduced into the Lagrangian formalism.³⁶⁻³⁷

Furthermore, we assume a robust DW structure described by $\mathbf{n} = (\text{sech}((z - q)/\lambda) \cos \Phi,$

$\text{sech}((z - q)/\lambda)\sin\Phi$, $\tanh((z - q)/\lambda)$,³⁶ where the azimuthal angle of the DW Φ are introduced as the collective coordinates. After substituting the DW ansatz and applying the Euler-Lagrange equation, we obtain the equation of motion for q and Φ ,

$$\frac{\rho^2}{\lambda A_0} \ddot{q} + \frac{\alpha \rho}{\lambda} \dot{q} + \frac{d\varepsilon}{dq} - \gamma \rho h = 0, \quad (8)$$

and

$$\frac{\rho^2}{A_0} \ddot{\Phi} + \alpha \rho \dot{\Phi} = 0. \quad (9)$$

It's noted that in Eq. 8, the first term describes the inertia of the DW and others represent the forces exerted by the damping, the pinning potential $\varepsilon(q)$ and the current-induced effective field, respectively. By substituting the initial condition $\Phi(0) = d\Phi/dt|_{t=0} = 0$ into Eq. 9, $\Phi(t) = 0$ is obtained, consistent with the fact that the AFM DW is confined in the easy plane due to the antiparallel arrangement of neighboring spins. For simplicity, we assume a parabolic potential^{23,29}

$$\varepsilon(q) = \begin{cases} K_N q^2 / 2 & (|q| < L_N) \\ K_N L_N^2 / 2 & (|q| \geq L_N) \end{cases}, \quad (10)$$

where K_N is the elastic constant and L_N is the radius of the potential well. After substitutions and necessary simplification, the equation of motion for q is updated to

$$\ddot{q} + G\dot{q} + \omega_N^2 q - h_N = 0, \quad (11)$$

where $G = \alpha A_0 / \rho$, $h_N = \gamma A_0 \lambda h / \rho$, and $\omega_N = (\lambda A_0 K_N / \rho^2)^{1/2}$ is the natural angular frequency of the free harmonic oscillator. Noting that Eq. 11 describes the damping oscillation of the DW, one has the solution for $\alpha < \alpha_c = 2\rho^2 a \omega_N / J A_0$ representing the under-damped oscillation

$$q(t) = e^{-Gt} (C_1 \cos \omega_p t + C_2 \sin \omega_p t) + h_N / \omega_N^2, \quad (12)$$

where $\omega_p = (\omega_N^2 - G^2/4)^{1/2}$ is the oscillating angular frequency of the DW, and C_1, C_2 are integral constants depending on the initial condition. As demonstrated in Eq. 12, the displacement of the DW consists of the oscillatory part (A_S) and stationary part (q_{eq}),²⁹ and its maximum value is approximately given by

$$|\Delta q|_{\max} = A_S + q_{eq} = e^{-G \arctan(C_2/C_1)/\omega_p} \sqrt{C_1^2 + C_2^2} + h_N / \omega_N^2. \quad (13)$$

$\omega_p \approx \omega_N$ is obtained for $\alpha < \alpha_c$. In this case, since $|\Delta q|_{\max}$ decreases exponentially with α ,

larger external field is required to generate the DW displacement for the DW depinning. When $|\Delta q|_{\max}$ is larger than L_N , the DW depins from the notch. Noting that the parameters of the pinning potential including K_N and L_N are unknown in our theory, which can be reasonably estimated by fitting the simulated results based on Eq. 13. As shown in Fig. 3(b) which presents the simulated furthest position of the DW q_{\max} as a function of α , the results can be well fitted by Eq. 13, further confirming the validity of our theory.

Since the oscillating amplitudes C_1 and C_2 are proportional to h , the field-independent parameters $c_1 = C_2/C_1$, $c_2 = (C_1^2 + C_2^2)^{1/2}/h$ are introduced for brevity. Subsequently, we estimate the depinning field under the condition $|\Delta q|_{\max} = L_N$,

$$h_{\text{dep}} = \frac{L_N}{e^{-G \arctan c_1 / \omega_p} c_2 + \gamma \rho / K_N}. \quad (14)$$

Similar fitting approach can be used to estimate L_N . As shown in Fig. 2(d), the simulated results and the theoretical results coincide with each other perfectly, demonstrating the important role of the internal DW dynamics in the DW pinning.

It is well known that the performance of the DW based racetrack memory not only depends on the velocity of the DW motion, but also relies on the DW depinning time. Thus, we also discuss the distinction between the depinning times of FM DWs and AFM DWs. In FM system, the oscillation of the DW position is related to the DW internal angle which is mainly determined by the internal fields including the anisotropy and Dzyaloshinskii-Moriya (DM) exchange fields.²⁷ Generally, the depinning time is inversely proportional to the magnitude of the internal fields and has a typical value of 10^{-9} s.^{22-24,27} However, in AFM system, the DW oscillation stems from the second-order derivative with respect to time rather than the azimuthal angle of the DW, as clearly illustrated in Eq. 8. Since the derivative is derived from the strong AFM exchange interaction between two sublattices which is about three orders larger than the anisotropy and DM fields, the depinning time in AFM systems has the magnitude of 10^{-12} s for typical antiferromagnets. As a result, the depinning time of AFM DW is three orders shorter than that of FM DW, indicating again the ultrafast AFM dynamics in the DW depinning.

In conclusion, we study the DW pinning at a notch in AFM nanowires theoretically and numerically. The depinning field depending on the notch size and internal parameters is

derived theoretically and confirmed by numerical simulations. Furthermore, the dependence of the depinning field on the damping constant is revealed, which is well explained by the analytical calculation on one-dimensional model considering the internal dynamics of the AFM DW. More interestingly, our work demonstrates a different depinning mechanism of the AFM DW and suggests that the depinning could be three orders faster than that of FM DW, further confirming the ultrafast dynamics of AFM systems.

Acknowledgment

The work is supported by the National Key Projects for Basic Research of China (Grant No. 2015CB921202), and the Natural Science Foundation of China (No. 11204091), and the Science and Technology Planning Project of Guangdong Province (Grant No. 2015B090927006), and the Natural Science Foundation of Guangdong Province (Grant No. 2016A030308019).

References:

1. O. Gomonay, V. Baltz, A. Brataas, and Y. Tserkovnyak, Nat. Phys. 14, 213 (2018).
2. A. V. Kimel, B. A. Ivanov, R. V. Pisarev, P. A. Usachev, A. Kirilyuk, and Th. Rasing, Nat. Phys. 5, 727 (2009).
3. N. T. Kühn, D. Schick, N. Pontius, C. Trabant, R. Mitzner, K. Holldack, H. Zabel, A. Föhlisch, and C. S. Langeheine, Phys. Rev. Lett. 119, 197202 (2017).
4. M. J. Grzybowski *et al.*, Phys. Rev. Lett. 118, 057701 (2017).
5. I. Fina, X. Martí D. Yi, J. Liu, J. H. Chu, C. R. Serrao, S. Suresha, A. B. Shick, J. Železný, T. Jungwirth, J. Fontcuberta, and R. Ramesh, Nat. Commun. 5, 4671 (2014).
6. P. Wadley *et al.*, Science 351, 587 (2016).
7. X. Z. Chen, R. Zarzuela, J. Zhang, C. Song, X. F. Zhou, G. Y. Shi, F. Li, H. A. Zhou, W. J. Jiang, F. Pan, and Y. Tserkovnyak, Phys. Rev. Lett. 120, 207204 (2018).
8. J. Železný, H. Gao, K. Výborný, J. Zemen, J. Mašek, A. Manchon, J. Wunderlich, J. Sinova, and T. Jungwirth, Phys. Rev. Lett. 113, 157201 (2014).
9. O. Gomonay, T. Jungwirth, and J. Sinova, Phys. Rev. Lett. 117, 017202 (2016).
10. Y. L. Zhang, Z. Y. Chen, Z. R. Yan, D. Y. Chen, Z. Fan, and M. H. Qin, Appl. Phys. Lett. 113, 112403 (2018).
11. E. G. Tveten, A. Qaiumzadeh, and A. Brataas, Phys. Rev. Lett. 112, 147204 (2014).
12. A. Qaiumzadeh, L. A. Kristiansen, and A. Brataas, Phys. Rev. B 97, 020402(R) (2018).
13. S. K. Kim, O. Tchernyshyov, and Y. Tserkovnyak, Phys. Rev. B 92, 020402(R) (2015).
14. S. Selzer, U. Atxitia, U. Ritzmann, D. Hinzke, and U. Nowak, Phys. Rev. Lett. 117, 107201 (2016).
15. Z. R. Yan, Z. Y. Chen, M. H. Qin, X. B. Lu, X. S. Gao, and J. –M. Liu, Phys. Rev. B 97, 054308 (2018).
16. T. Shiino, S. Oh, P. M. Haney, S. Lee, G. Go, B. Park, and K. Lee, Phys. Rev. Lett. 117, 087203 (2016).
17. S. K. Kim, D. Hill, and Y. Tserkovnyak, Phys. Rev. Lett. 117, 237201 (2016).
18. Z. Y. Chen, Z. R. Yan, Y. L. Zhang, M. H. Qin, Z. Fan, X. B. Lu, X. S. Gao, and J. –M. Liu, New J. Phys. 20, 063003 (2018).

19. P. Wadley *et al.*, Nat. Nanotechnol. 13, 362 (2018).
20. D. A. Allwood, G. Xiong, C. C. Faulkner, D. Atkinson, D. Petit, R. P. Cowburn, Science 309, 1688 (2005).
21. S. S. P. Parkin, U.S. Patent No. 6,834,005 (2004).
22. S. S. P. Parkin, M. Hayashi, and L. Thomas, Science 320, 190 (2008).
23. L. Thomas, M. Hayashi, X. Jiang, R. Moriya, C. Rettner, and S. S. P. Parkin, Nature 443, 197 (2006).
24. L. Thomas, M. Hayashi, X. Jiang, R. Moriya, C. Rettner, and S. Parkin, Science 315, 1553 (2007).
25. M. Hayashi, L. Thomas, C. Rettner, R. Moriya, X. Jiang, and S. S. P. Parkin, Phys. Rev. Lett. 97, 207205 (2006).
26. H. Y. Yuan and X. R. Wang, Phys. Rev. B 89, 054423 (2014).
27. S. Moretti, M. Voto, and E. Martinez, Phys. Rev. B 96, 054433 (2017).
28. E. Martinez, L. Lopez-Diaz, O. Alejos, L. Torres, and C. Tristan, Phys. Rev. Lett. 98, 267202 (2007).
29. E. Martinez, L. Lopez-Diaz, O. Alejos, and L. Torres, Phys. Rev. B 77, 144417 (2008).
30. D. Ravelosona, D. Lacour, J. A. Katine, B. D. Terris, and C. Chappert, Phys. Rev. Lett. 95, 117203 (2005).
31. D. Bedau, M. Kläui, M. T. Hua, S. Krzyk, U. Rüdiger, G. Faini, and L. Vila, Phys. Rev. Lett. 101, 256602 (2008).
32. H. Y. Yuan and X. R. Wang, Phys. Rev. B 92, 054419 (2015).
33. E. G. Tveten, T. Muller, J. Linder, and A. Brataas, Phys. Rev. B 93, 104408 (2016).
34. K. M. Pan, L. D. Xing, H. Y. Yuan, and W. W. Wang, Phys. Rev. B 97, 184418 (2018).
35. J. J. Liang, J. H. Yu, J. Chen, M. H. Qin, M. Zeng, X. B. Lu, X. S. Gao, and J. –M. Liu, New J. Phys. 20, 053037 (2018).
36. K.-J. Kim, S. K. Kim *et al.*, Nat. Mater. 16, 1187 (2017).
37. S. K. Kim, Y. Tserkovnyak, and O. Tchernyshyov, Phys. Rev. B 90, 104406 (2014).

FIGURE CAPTIONS

Fig.1. (color online) Spin structures around the notch in the AFM nanowire with lattice sizes $l \times w \times t_l$ under (a) $h = 0$, (b) $h = 0.002J/\mu_S$, (c) $h = 0.004J/\mu_S$, and (d) $h = 0.0043J/\mu_S$. The color represents the magnitude of the z component of the staggered magnetization n_z .

Fig.2. (color online) Numerical (empty circles) and analytical (blue solid line) calculated depinning field as a function of (a) the depth of the notch w_N , (b) the width of the nanowire w , (c) the anisotropy constant d_z , and (d) the damping constant α . The red solid line in (d) is the fitting results based on Eq. 14.

Fig.3. (color online) (a) The DW position as a function of time for various damping constants under $h = 0.0039J/\mu_S$. (b) Numerical (empty circles) and analytical (solid line) calculated maximum displacement of the DW as a function of α under $h = 0.0039J/\mu_S$.

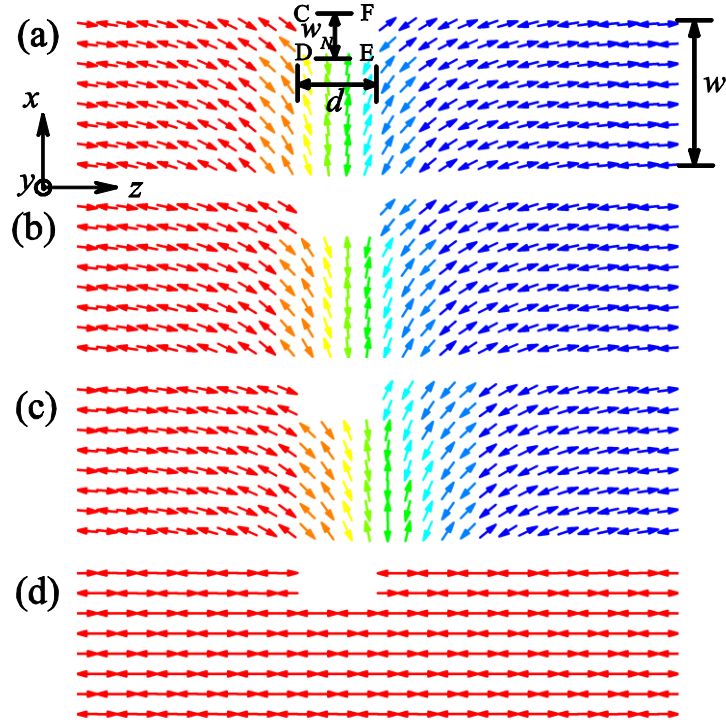


Fig.1. (color online) Spin structures around the notch in the AFM nanowire with lattice sizes $l \times w \times t_l$ under (a) $h = 0$, (b) $h = 0.002J/\mu_S$, (c) $h = 0.004J/\mu_S$, and (d) $h = 0.0043J/\mu_S$. The color represents the magnitude of the z component of the staggered magnetization n_z .

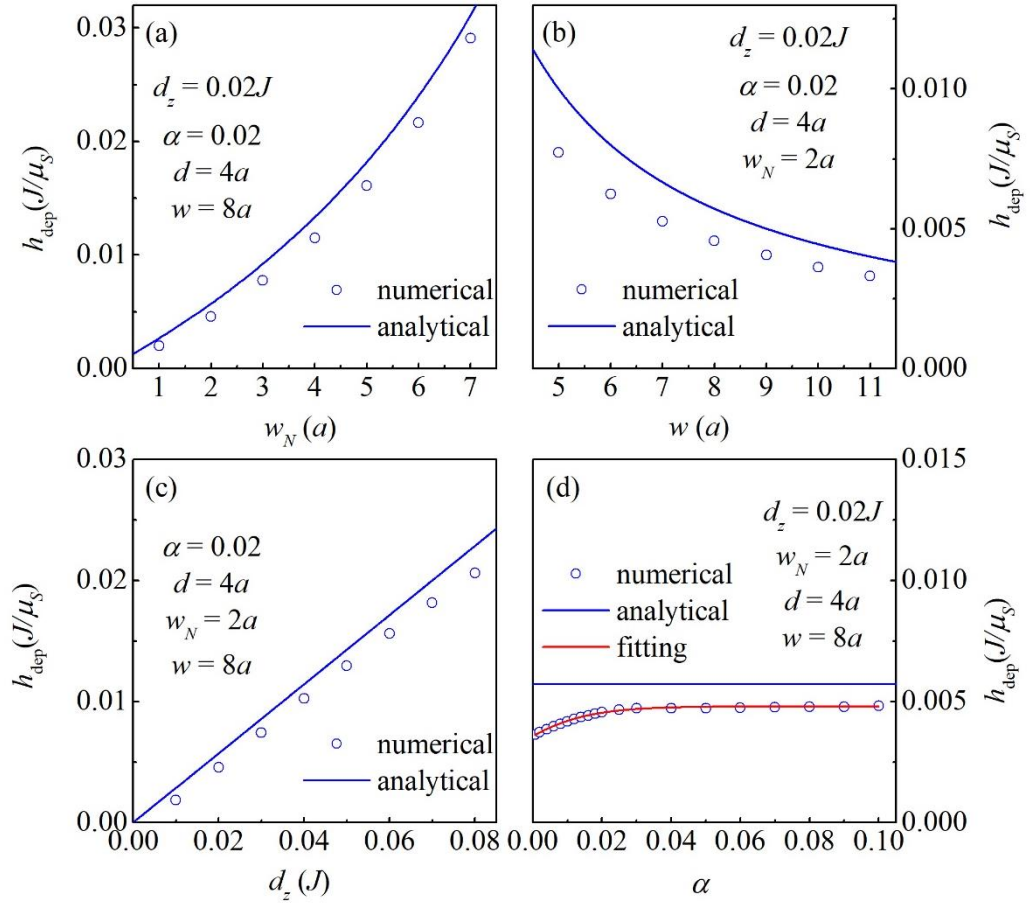


Fig.2. (color online) Numerical (empty circles) and analytical (blue solid line) calculated depinning field as a function of (a) the depth of the notch w_N , (b) the width of the nanowire w , (c) the anisotropy constant d_z , and (d) the damping constant α . The red solid line in (d) is the fitting results based on Eq. 14.

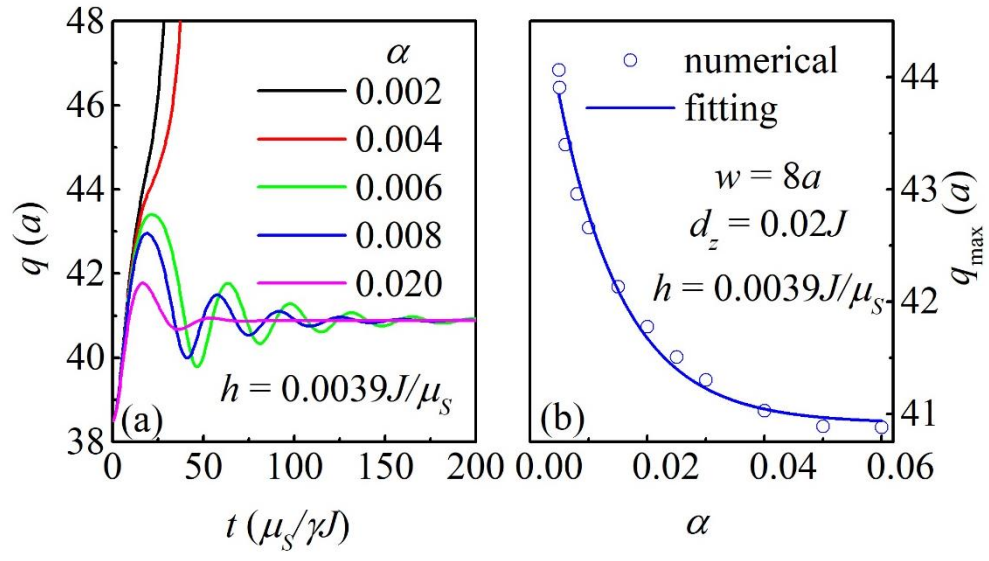


Fig.3. (color online) (a) The DW position as a function of time for various damping constants under $h = 0.0039J/\mu_s$. (b) Numerical (empty circles) and analytical (solid line) calculated maximum displacement of the DW as a function of α under $h = 0.0039J/\mu_s$.

Supplementary material for
“Depinning of domain walls in notched antiferromagnetic nanowires”

Z. Y. Chen¹, M. H. Qin^{1,*}, and J. -M. Liu²

¹*Institute for Advanced Materials, South China Academy of Advanced Optoelectronics and
Guangdong Provincial Key Laboratory of Quantum Engineering and Quantum Materials,
South China Normal University, Guangzhou 510006, China*

²*Laboratory of Solid State Microstructures and Innovative Center for Advanced
Microstructures, Nanjing University, Nanjing 210093, China*

A. Derivation of the depinning field

The model Hamiltonian density reads

$$H = \frac{A_0}{2} \mathbf{m}^2 + \frac{A}{2} \nabla \mathbf{n} \cdot \nabla \mathbf{n} + L_0 \mathbf{m} \cdot \nabla \mathbf{n} - \frac{K_z}{2} n_z^2 + h n_z. \quad (1)$$

After eliminating \mathbf{m} with $\mathbf{m} = -L_0 \nabla \mathbf{n} / A_0$, we obtain

$$H = \frac{A^*}{2} \nabla \mathbf{n} \cdot \nabla \mathbf{n} - \frac{K_z}{2} n_z^2 + \gamma \rho h n_z. \quad (2)$$

In the following, we use the same method with Ref. 24 to derive the depinning field for AFM DWs. At low temperatures, we introduce the Lagrange multiplier ξ to take into account the constraint condition $\mathbf{n} \cdot \mathbf{n} = 1$, and then construct a new function

$$F = \int dV \left(\frac{A^*}{2} \nabla \mathbf{n} \cdot \nabla \mathbf{n} + f_{ot} \right) - \xi (\mathbf{n} \cdot \mathbf{n} - 1), \quad (3)$$

where f_{ot} is the sum of the anisotropy and Zeeman energy. Using the variational method, we obtain

$$-l_{ex}^2 \nabla^2 n_i + \frac{\partial f_{ot}}{\partial n_i} + 2\xi n_i = 0, \quad (4)$$

where $l_{ex} = (aA^* / J)^{1/2}$ is the exchange length in AFM systems, n_i is the x_i component of \mathbf{n} (x_i

*qinmh@scnu.edu.cn

$= x, y, z$). To eliminate ξ , we take the product of Eq. 4 and sum over i and obtain

$$-l_{ex}^2 \frac{\partial n_i}{\partial x_j} \nabla^2 n_i + \frac{\partial f_{ot}}{\partial x_j} = 0. \quad (5)$$

Transforming Eq. 5 with the identity

$$\frac{\partial g}{\partial x_j} \nabla^2 g = \nabla \cdot \left(\frac{\partial g}{\partial x_j} \nabla g \right) - \frac{1}{2} \frac{\partial}{\partial x_j} (\nabla g)^2, \quad (6)$$

and we obtain

$$\frac{\partial}{\partial x_j} \left(\frac{1}{2} l_{ex}^2 \nabla n_i \cdot \nabla n_i + f_{ot} \right) = l_{ex}^2 \nabla \cdot \left(\frac{\partial n_i}{\partial x_j} \nabla n_i \right). \quad (7)$$

To eliminate the space-dependent variables, we take the summation over the whole regions of the sample Ω ,

$$\int_{\Omega} dV \frac{\partial}{\partial x_j} \left(\frac{1}{2} l_{ex}^2 \nabla n_i \cdot \nabla n_i + f_{ot} \right) = \int_{\Omega} dV l_{ex}^2 \nabla \cdot \left(\frac{\partial n_i}{\partial x_j} \nabla n_i \right) = \int_{\partial\Omega} d\mathbf{S} \cdot l_{ex}^2 \frac{\partial n_i}{\partial x_j} \nabla n_i, \quad (8)$$

where $\partial\Omega$ is the boundary of Ω . Considering the boundary condition $\nabla n_i = 0$, we have

$$\int_{\Omega} dV \frac{\partial}{\partial z} \left(\frac{1}{2} l_{ex}^2 \nabla n_i \cdot \nabla n_i + f_{ot} \right) = \int_{GH-EF+CD-AB} dx dy \left(\frac{1}{2} l_{ex}^2 \nabla n_i \cdot \nabla n_i + f_{ot} \right) = 0. \quad (9)$$

Substituting the configuration of the system into Eq. 9 and we obtain

$$t_l \int_{CD-EF} dy \left(\frac{1}{2} l_{ex}^2 \nabla n_i \cdot \nabla n_i + f_{ot} \right) = -2ht_l w. \quad (10)$$

Then the magnitude of the current-induced effective field is given by

$$h = \frac{t_l \int_{CD-EF} dy \left(\frac{1}{2} l_{ex}^2 \nabla n_i \cdot \nabla n_i + f_{an} \right)}{t_l w_N (2w / w_N + \langle n_{zEF} \rangle - \langle n_{zCD} \rangle)}, \quad (11)$$

where $\langle n_{zEF} \rangle$, $\langle n_{zCD} \rangle$ are the average z components of \mathbf{n} on surfaces EF and CD , respectively.

The depinning field represents the minimum field to move a DW, and in other words, the maximum field that Eq. 11 has a stationary solution. Thus, critical condition is the key to deriving the depinning field. Similar to the earlier work, we consider the critical condition $\langle n_{zEF} \rangle = 0$, $\langle n_{zCD} \rangle = 1$ in our derivation, whose validity is confirmed in Fig. 1(c) in the manuscript. After substitutions and simplifications, we obtain the depinning field of AFM

DWs

$$h_{dep} = \frac{2d_z / \mu_s}{2w / w_N - 1} . \tag{12}$$